PREPRINT NO. 1038 (F-3)

WHAT'S SO SACRED ABOUT EXPONENTIAL HORNS?

BY

D. B. KEELE, JR.
ELECTRO-VOICE, INC.
BUCHANAN, MICHIGAN

PRESENTED AT THE

51st CONVENTION

MAY 13-16, 1975

AN AUDIO ENGINEERING SOCIETY PREPRINT

WHATS SO SACRED ABOUT EXPONENTIAL HORNS?

D. B. Keele, Jr.
Electro-Voice, Inc.
Buchanan, Michigan 49107

The maintenance of constant directivity with frequency in high-frequency exponential horns is quite difficult. Two main sound industry solutions are the multicell and radial/sectoral horns. While the multicell exhibits fairly constant directivity, both designs suffer from mid/high-frequency polar lobing and midrange narrowing, and the radial shows continually decreasing vertical beamwidth as frequency increases. A new series of horns which optimally joins a modified conical horn with an exponential throat section corrects these problems, while offering very well behaved polar patterns and constant directivity up to 16 kHz.

INTRODUCTION:

Horns are used in sound systems primarily for two reasons: (1) high efficiency (and the resultant high acoustic output with low distortion) and (2) pattern/coverage control. The ideal horn should have constant directivity and coverage angle and provide a constant acoustic load to the driver at all frequencies in the designed operating range of the horn. Up to now, these goals were for the most part met by designs based on exponential horn theory. The exponential horn was found to be particularly effective in providing good response right down to horn cutoff, especially for the hyperbolic-exponential designs [1].

Unfortunately the exponential horn in its purist form is not conducive to control of beamwidth and directivity. The directional characteristics of the exponential horn are found to be highly dependent on the flare rate [2, p. 487]. To get around this problem two main horn designs have surfaced:

(1) the multicellular horn and (2) the radial/sectoral horn. Both these designs in one way or the other attempt to simulate an acoustic source which is the analog of a portion of a pulsating sphere. This is a result of acoustic theory which states [2], p. 507:

> "A portion of a spherical surface large compared to wavelength and vibrating radially, emits uniform sound radiation over a solid angle subtended by the surface at the center of curvature. To obtain uniform sound distribution over a certain solid angle, the radial air motion must have the same phase and amplitude over the spherical surface intercepted by the angle having its center of curvature at the vertex and the dimensions of the surface must be large compared to wavelength. When these conditions are satisfied for all frequencies, the response will be independent of the position within the solid angle."

The perfect pulsating sphere segment provides quite good constant beamwidth high frequency (dimensions much larger than wavelength) polars but is found to suffer from a couple of defects of its own. In the frequency range where the wavelength is comparable to segment size, the polar pattern gets quite narrow and sometimes collapses to some 40 to 50% of the high frequency beamwidth [2], p. 40-42, p. 507. In addition, above this frequency, the sphere segment radiation exhibits moderate lobing and fingering in the polar response.

The multicell and radial horn designs are only moderately successful in simulating the radially vibrating sphere surface. As a result, their directional characteristics exhibit some of the defects of the sphere radiation along with some defects of their own.

On first examination the conical horn appears to have excellent potential in simulating the sphere segment because of its inherent constant solid angle configuration, but unfortunately its poor low frequency performance has kept designers from using it. This paper describes the design of a new class of loudspeaker horns based on an optimal joining of modified conical and exponential flares. This horn design exhibits the excellent pattern control of the conical, but without the midrange narrowing and HF lobing, and the good low frequency response of the exponential.

THE IDEAL HORN:

As stated in the introduction, the ideal horn should have constant directivity and beamwidth as a function of frequency and provide a constant acoustic load to the driver. A real world horn, being of finite size, offers directivity control only down to that frequency where the wavelength is comparable to horn mouth size. Below this frequency, the beamwidth increases

monotonically (roughly doubling for each halfing of frequency up to 360° where the horn then becomes an omnidirectional source). Beamwidth is defined in this paper as the total included angle between the directions at which the sound pressure level (SPL) is down 6 dB from the on axis reference direction.

Fig. 1 illustrates the beamwidth vs. frequency (in one plane only) for a hypothetical ideal horn providing a pie slice polar response with coverage angle θ_I.[1] Note that the beamwidth is constant down to f_T and then roughly doubles for each octave decrease in frequency. The intercept frequency f_T is the point where the asymtote to the beamwidth curve for low frequencies ($f < f_T$) crosses the rated beamwidth angle. f_T is roughly that frequency where horn size is comparable to wavelength. Fig. 2 likewise shows the beamwidth for a hypothetical ideal rectangular coverage horn radiating into a solid cone of space with angles θ_H by θ_V [3, p. 1127]. Physical size constraints, discussed later in this paper, govern the ordering of the intercept frequencies i.e. if $\theta_H > \theta_V$ then $f_{IV} > f_{IH}$.

Fig. 3 shows the directivity index D_I [3, p. 1097] vs. frequency for the same hypothetical rectangular coverage horn. Above the upper intercept frequency f_{IV} the directivity is constant. For low frequencies ($f < f_{IH}$) the directivity increases at a rate of up to 6 db per octave. Between f_{IH} and f_{IV} the directivity rises at 3 db per octave.

EXISTING DESIGN PROBLEMS:
Radial Horn:

A conventional radial/sectoral horn design is shown pictorially in Fig. 4. The exponential flare is created by straight sides on two boundaries and curved sides on the other two boundaries [2, p. 507]. Typical polar patterns for this horn are shown in Fig. 5. Typical beamwidth and directivity curves are shown respectively in Figs. 6 and 7.

An examination of Figs. 5, 6 and 7 reveals several performance problems with the radial design. Note the midrange horizontal beamwidth narrowing around 1.25 kHz. Observe the continual decrease in vertical beamwidth with increasing frequency. The effects of polar lobing on beamwidth are indicated in Fig. 6 by the non constant horizontal beamwidth between 2 kHz and 10 kHz. The relatively large throat dimension (X-X in Fig. 4) makes itself evident in the eventual decrease of horizontal high frequency beamwidth and the continually rising directivity (Figs. 6 and 7).

[1] The pie slice or wedge shape certainly is not the ideal polar pattern for all applications. For a source elevated above a flat plane, a source whose vertical strength varies inversely as the sin of the off-axis angle would compensate precisely for the inverse level with distance law.

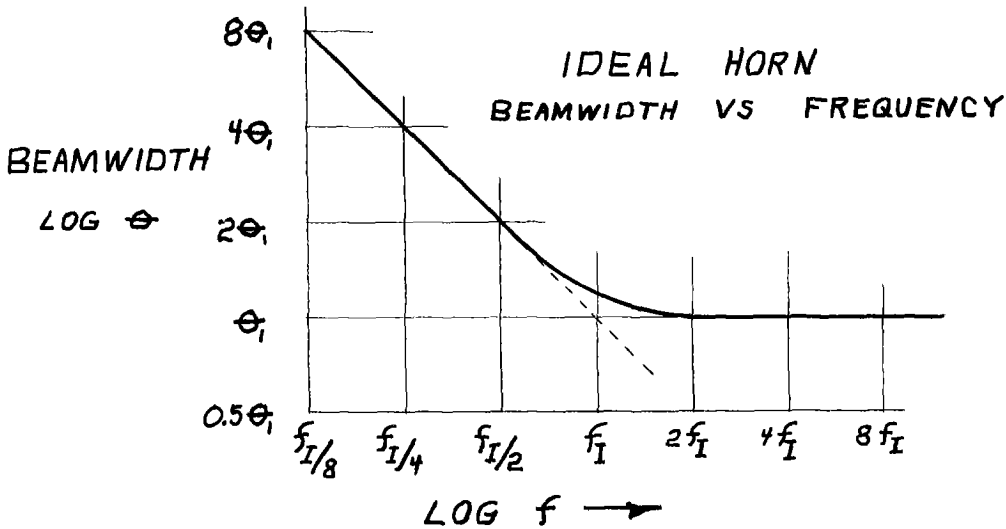

Fig. 1. Beamwidth versus frequency for a hypothetical ideal horn. The beamwidth is constant at θ, above f_I and roughly doubles for each octave decrease in frequency below f_I. For very low frequencies, the beamwidth attains 360° where the horn radiates omnidirectionally.

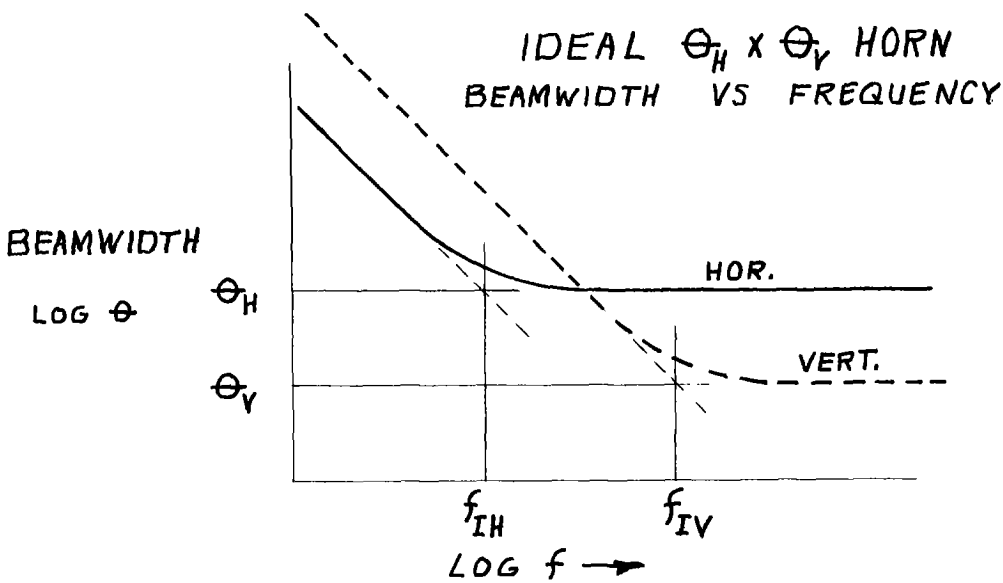

Fig. 2. Beamwidth versus frequency for an ideal rectangular coverage horn that provides a θ_H (hor.) by θ_V (vert.) radiation pattern.

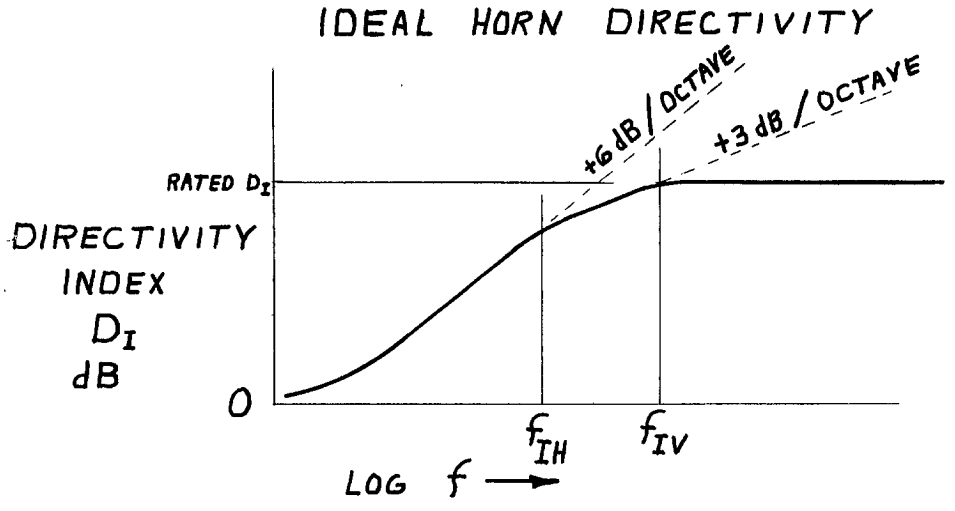

Fig. 3. Directivity index D_I (= 10 log R_θ) as a function of frequency for the ideal rectangular coverage horn of Fig. 2.

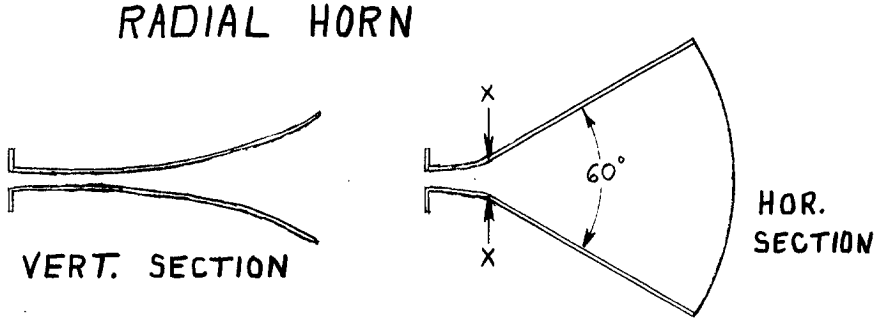

Fig. 4. Sketch of a typical 60° horizontal coverage angle exponential radial/sectoral horn. The horizontal section expands with straight sidewalls angled at 60°, while the exponential taper is provided by the curved vertical boundaries. The following experimental measurements shown in Figs. 5 to 7 were made on a 60° radial horn with overall dimensions of 20.3 cm(8 in.) mouth height, 61.3 cm(24.1 in.) mouth width and 50.8 cm(20 in.) length.

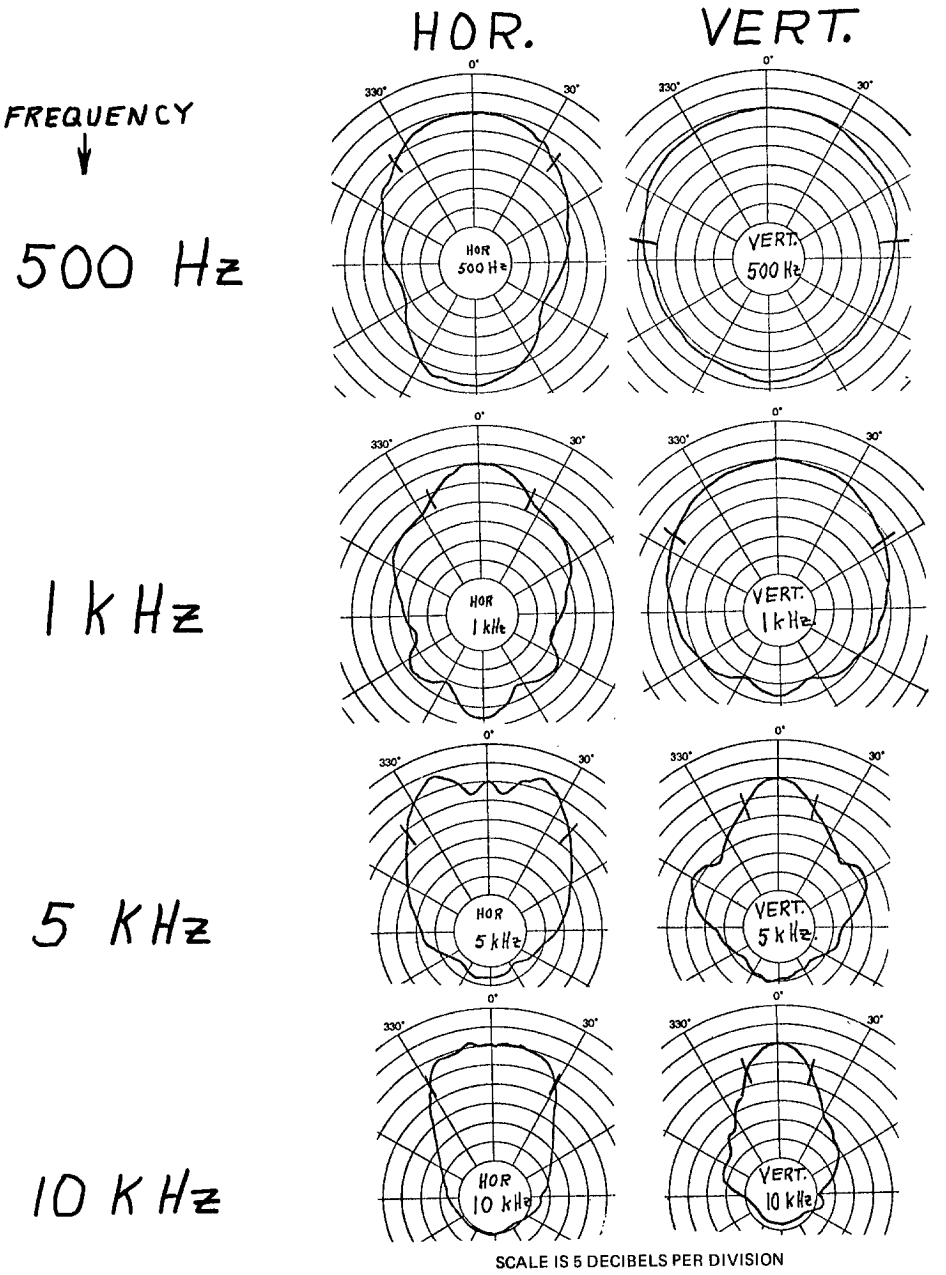

Fig. 5. Some selected one-third octave bandwidth polar responses (3 meters from mouth) measured on the 60° radial horn discribed in Fig. 4. Note the narrow 42° horizontal beamwidth at 1 kHz and the horizontal lobing at 5 kHz.

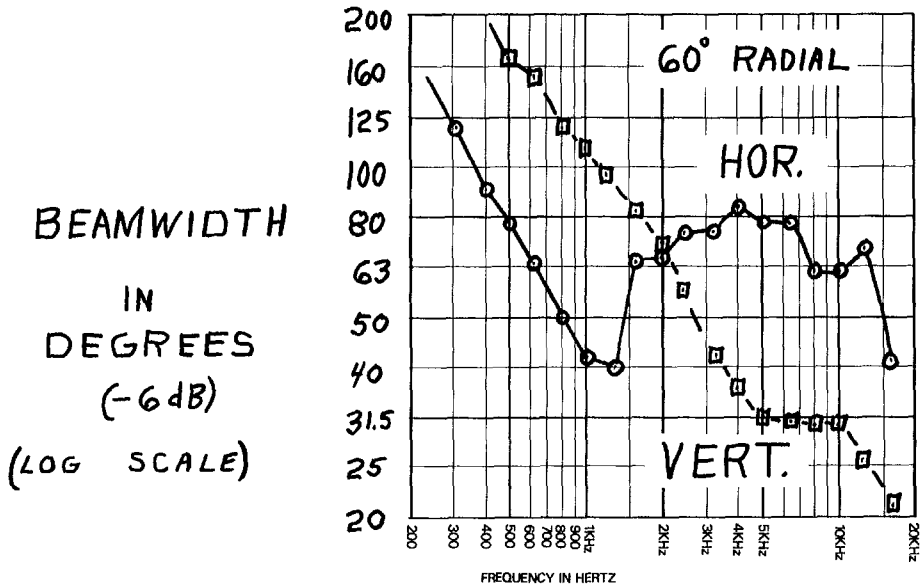

Fig. 6. Beamwidth (-6 dB) plotted against frequency for the 60° radial horn discribed in Fig. 4. The angular coverage of this horn is rated at 60° x 40° by the manufacturer. These measurements were taken from a complete set of one-third octave polar curves measured in EV's anechoic chamber. Observe the horizontal narrowing around 1.25 kHz and the steadily falling vertical beamwidth with frequency.

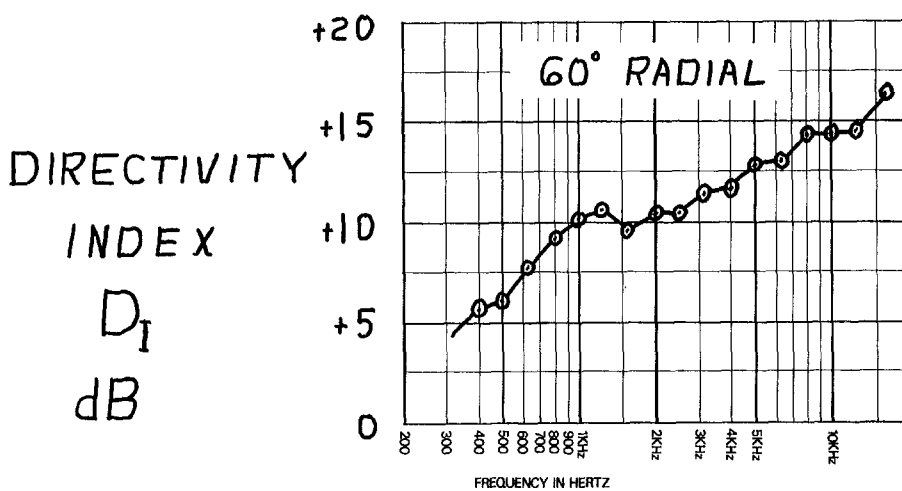

Fig. 7. Directivity index D_I vs. frequency for the 60° radial horn of Fig. 4. Notice the steady rise as frequency increases. The ideal rectangular 60° x 40° coverage angle horn, with wedge shaped polar patterns, would have a D_I of +12.6 dB.

Multicellular Horn:

The multicell is depicted in Fig. 8 [2, p. 517]. This horn consists of a large number of small exponential horns with axis passing through a common point. This assemblage in the low and mid frequencies effectively simulates a spherical surface of uniform phase and amplitude at the mouths of the horns. At higher frequencies above 6 kHz, however, each horn independently radiates a narrower beam. This gives rise to severe ripples in the HF polar response as one goes on and off axis of each individual horn. Fig.s 9 to 11 illustrate some typical measurements on this type of horn (an Electro-Voice M253 2 x 5 cell). Note that the multicell exhibits the midrange narrowing effect in both horizontal and vertical planes. Beranek [3, p. 1087] displays some beamwidth versus frequency curves for the multicell which show the midband narrowing effect in more detail.

WHAT TO DO?

Assuming the designer wants to simulate the pulsating sphere section more closely, is there another type of horn flare other than exponential which would work better? The answer is yes and that flare turns out to be the conical (Fig. 12). Unfortunately, the low frequency response of the conical horn is quite poor. In comparison to an exponential horn of the same overall dimensions, the conical horn has much less output in the first two octaves of operation. Fig. 13 compares the efficiency of the two horn types when each is driven by a matched acoustic source (see appendix 1).

Disregarding the low frequency efficiency problem, the conical horn is found to be very conducive to designs that require uniform coverage in a specific solid angle. The constant solid angle configuration of the conical horn precisely fits the requirements noted in the paragraph quoted in the introduction of this paper. In addition, the conical horn can be made large without limit and not incur destructive mouth reflections back into the horn as is exhibited by the exponential horn [4]. This latter characteristic of the conical horn allows the designer to optimise coverage versus frequency by increasing the horn's length and size, without fear of degrading response.

A SOLUTION:

Research done for a previous paper [4], which dealt with selection of an optimum exponential horn mouth size for radiation into fractional solid angle spaces ($\Psi < 2\pi$), suggested to the author an optimum way to join an exponential flare and conical flare together in the same horn (see appendix 2).[2]

[2]The author is indebted to his former boss at Electro-Voice, John Gilliom, for first recognizing that this combination would be useful and for construction of a working model.

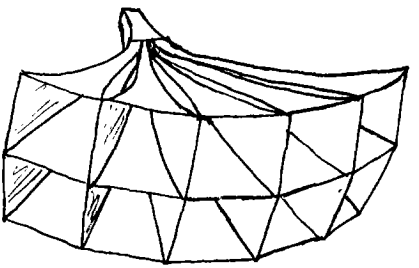

Fig. 8. Sketch of a typical multicellular exponential horn. This unit is the 2 x 5 cell Electro-Voice model M253 with overall dimensions of 44.5 cm(17.5 in.) mouth height, 92.7 cm(36.5 in.) mouth width and 53.8 cm(21.2 in.) length.

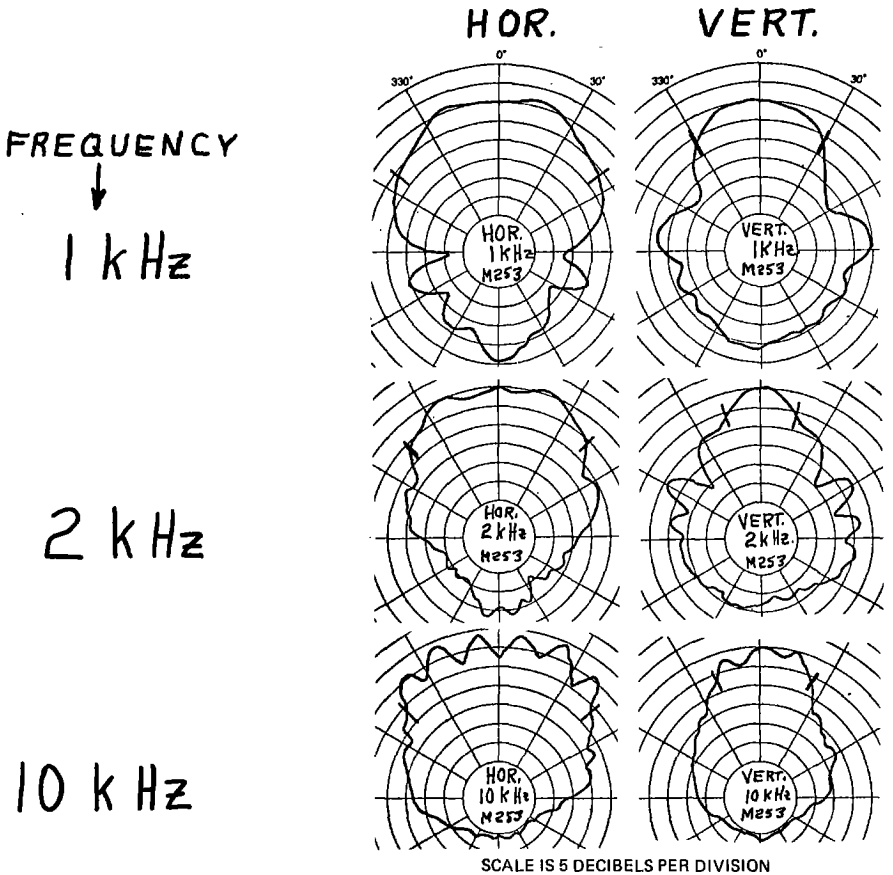

Fig. 9. Selected one-third octave polar measurements on the 2 x 5 multicell of Fig. 8. Note the lobing and fingering in all the polars and the narrow vertical curve at 2 kHz.

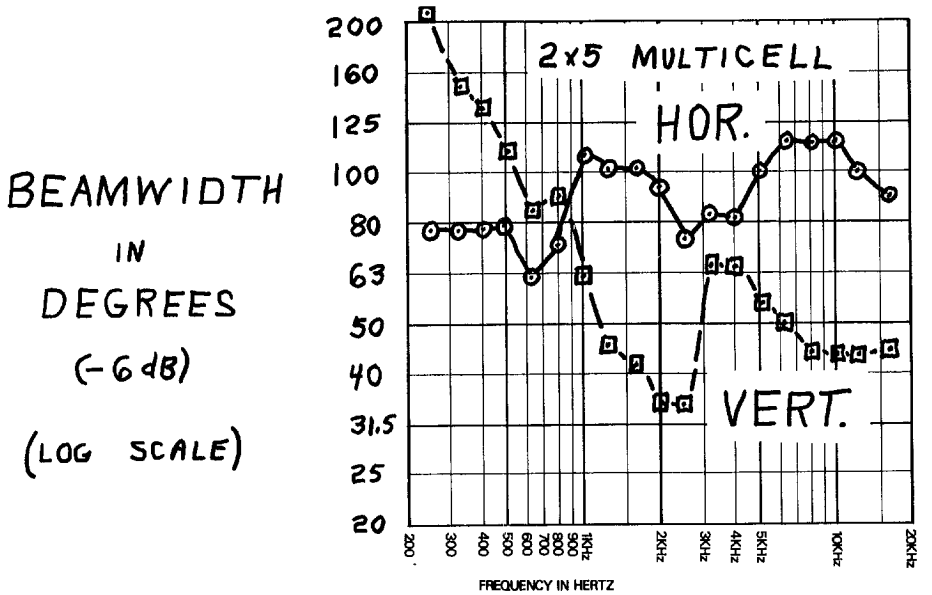

Fig. 10. Beamwidth versus frequency for the 2 x 5 multicell discribed in Fig. 8. The manufacturer rates this horn as covering 120^{o} x 60^{o}. Observe the decrease in beamwidth at 630 Hz (hor.) and 2 kHz (vert.)

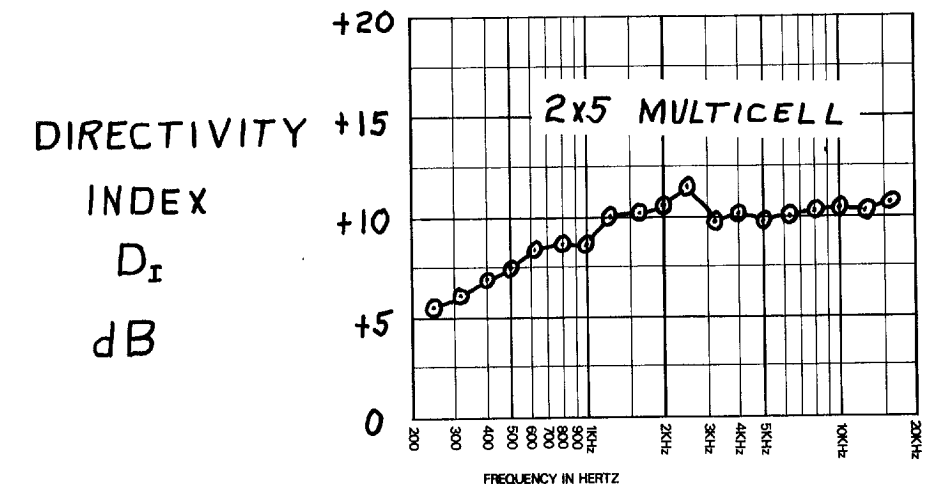

Fig. 11. Directivity index D_I against frequency for the 2 x 5 multicell of Fig. 8. The typically uniform directivity above 800 Hz explains why the multicell has seen such wide usage in sound systems over the years.

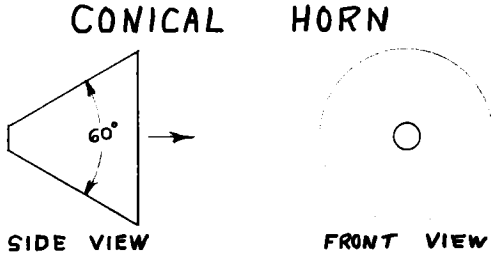

Fig. 12. A 60° circular crossection conical horn (otherwise known as a megaphone). The conical taper is the only one which provides a constant solid angle to wavefronts traveling through the horn.

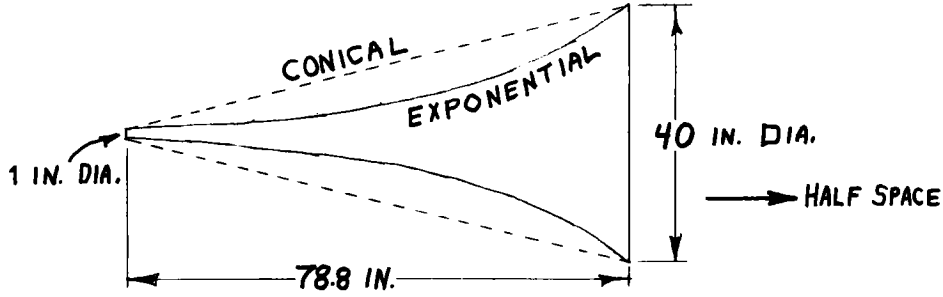

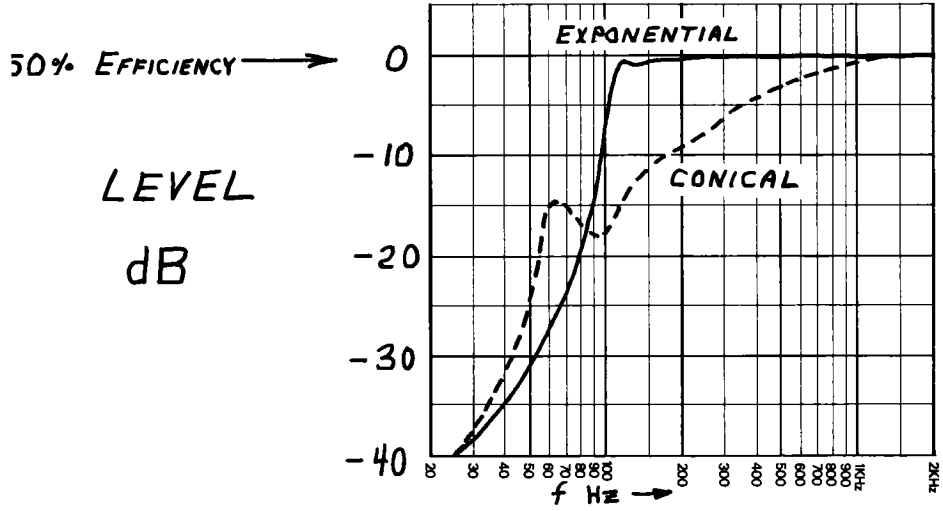

Fig. 13. Efficiency comparison between an exponential and conical horn with the same overall dimensions when driven by the matched acoustical source (see appendix 1). Observe the poor conical response between 100 and 500 Hz. The exponential has a cutoff frequency of 100 Hz and an optimum size mouth ($k_c a_M = 0.93$, see [47]) for radiation into the half-space load. The radiation impedance for the half-space environment is modeled by a piston (same diameter as horn's mouth) in an infinite flat plane.

This composite flare horn would be an exponential in the first portion and conical thereafter (Fig. 14). This new combination exhibits the good low frequency response of the exponential and the excellent coverage control of the conical.

Fig. 15 shows response comparisons between different sized exponential and composite conical-exponential horns (hereafter called the CE horn) all with the same cutoff frequency and throat diameter. In comparison with an exponential horn of the same mouth/throat size and equivalent low frequency performance, the CE horn is found to be roughly 10 to 40% longer (length depends on selected coverage angle):

MIDRANGE NARROWING:

The newly designed CE horn is not without its own problems, however. The polar narrowing effect, when the horn mouth is roughly comparable to wavelength, still exists. Also, the polar lobing and fingering characteristic of the sphere segment radiation is also exhibited. An imperically derived solution to these problems was found in a secondary rapid flaring near the mouth of the CE horn (Fig. 16). The secondary flaring, in addition to solving the narrowing problem, was found also to considerably reduce the lobing and fingering in the polar response.

Good results were obtained when roughly the last third of the conical horn sidewall was displaced outward so as to double the included angle (Fig. 16). On first thought, this increase in physical mouth size would seem to have the effect of narrowing the beamwidth even further. However, measurements of amplitude across the horn mouth show that the effective acoustic source size actually decreases, because the amplitude is much higher in the center of the horn than on the outside edges (these comments only apply to the frequency range where the wavelength is comparable to mouth size, at higher frequencies the amplitude is again roughly constant over the horn mouth).

ANGLE-SIZE-FREQUENCY TRADEOFFS:

For a specific desired coverage angle and intercept frequency, how large must the horn be? An imperically derived relationship was found to hold for these variables (Fig. 17, also see Fig. 1):

$$X = \frac{K}{\theta f_I} \qquad (1)$$

where,

X = horn mouth width,

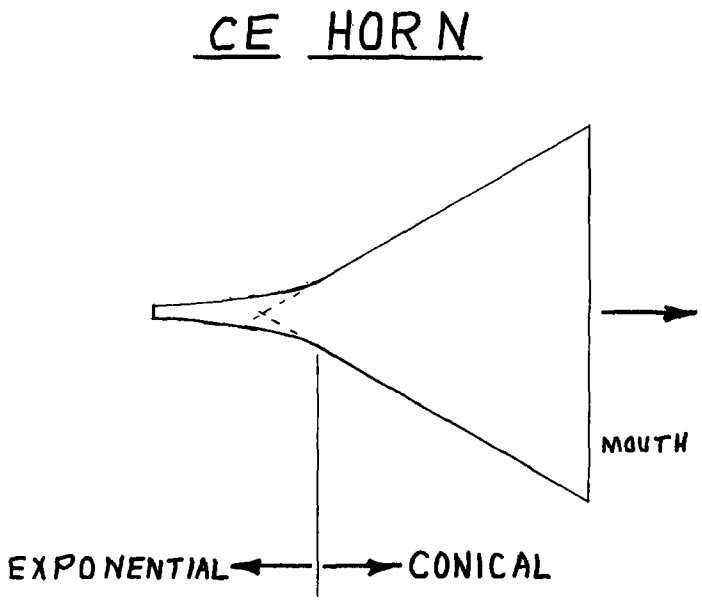

Fig. 14. A multiflare horn combining exponential and conical flares. The boundary point between the two flares should be selected to minimize junction reflections.

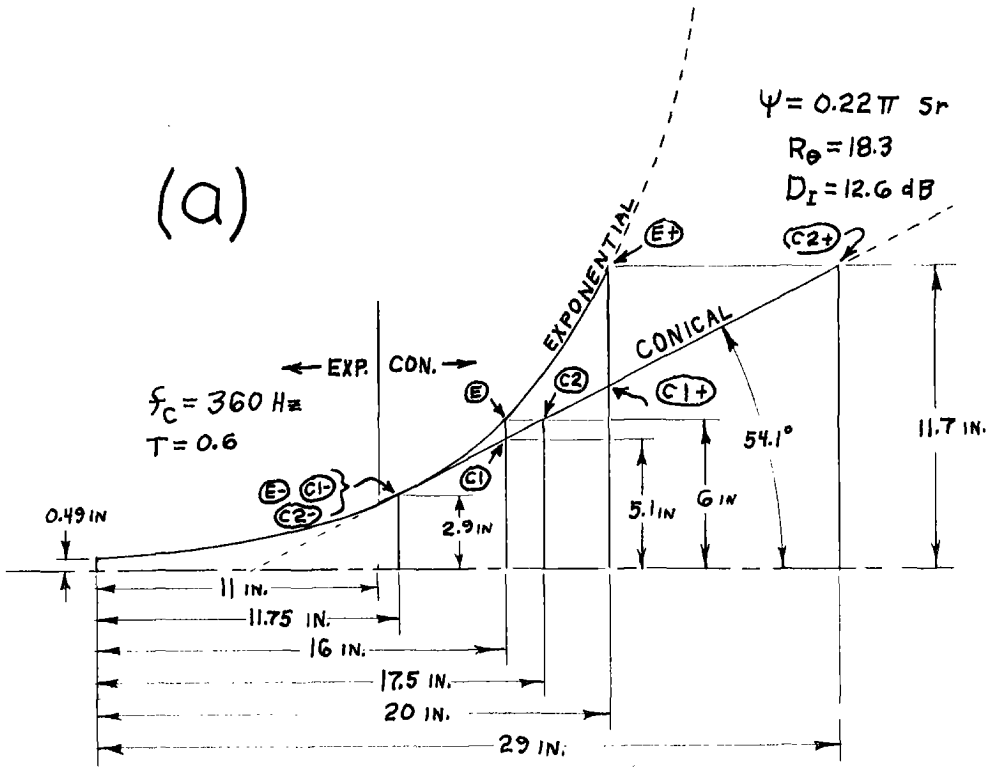

Fig. 15. Efficiency versus frequency comparisons of several different sized exponential and composite conical-exponential horns (CE horn) using the matched acoustic source (appendix 1). All of these horns are developed from the same circular crossection hyperbolic-exponential prototype horn with cutoff f_c = 360 Hz, T = 0.6 and throat diameter of 0.98 inch (a). The solid angle Ψ of the added conical section is equal to that provided by a perfect 60° x 40° coverage angle horn. The optimum transition from exponential to conical flares occurs at 11 inches from the start of the horn.

Three different sized exponential prototype horns are considered which are centered about the optimum size (47). Mouth diameter ratios of one-half optimum (E-) ($k_c a_M$ = 0.5), optimum (E) ($k_c a_M$ = 1) and twice optimum (E+) ($k_c a_M$ = 2) are analyzed. For each of these prototype exponentials, two conical-exponential horns are generated: 1 a CE horn which has the same length as the exponential prototype but with a smaller mouth size and (2) a CE horn which has the same mouth diameter but is longer than its corresponding exponential prototype. These horns are designated respectively (C1-) (C2-) for the (E-) prototype, (C1) (C2) for the (E) prototype and (C1+) (C2+) for the (E+) prototype.

These nine horns are depicted in (a) with all relevant dimensions shown. Only the sidewall contour is shown; the complete horn is developed by rotation of this curve about the center line.

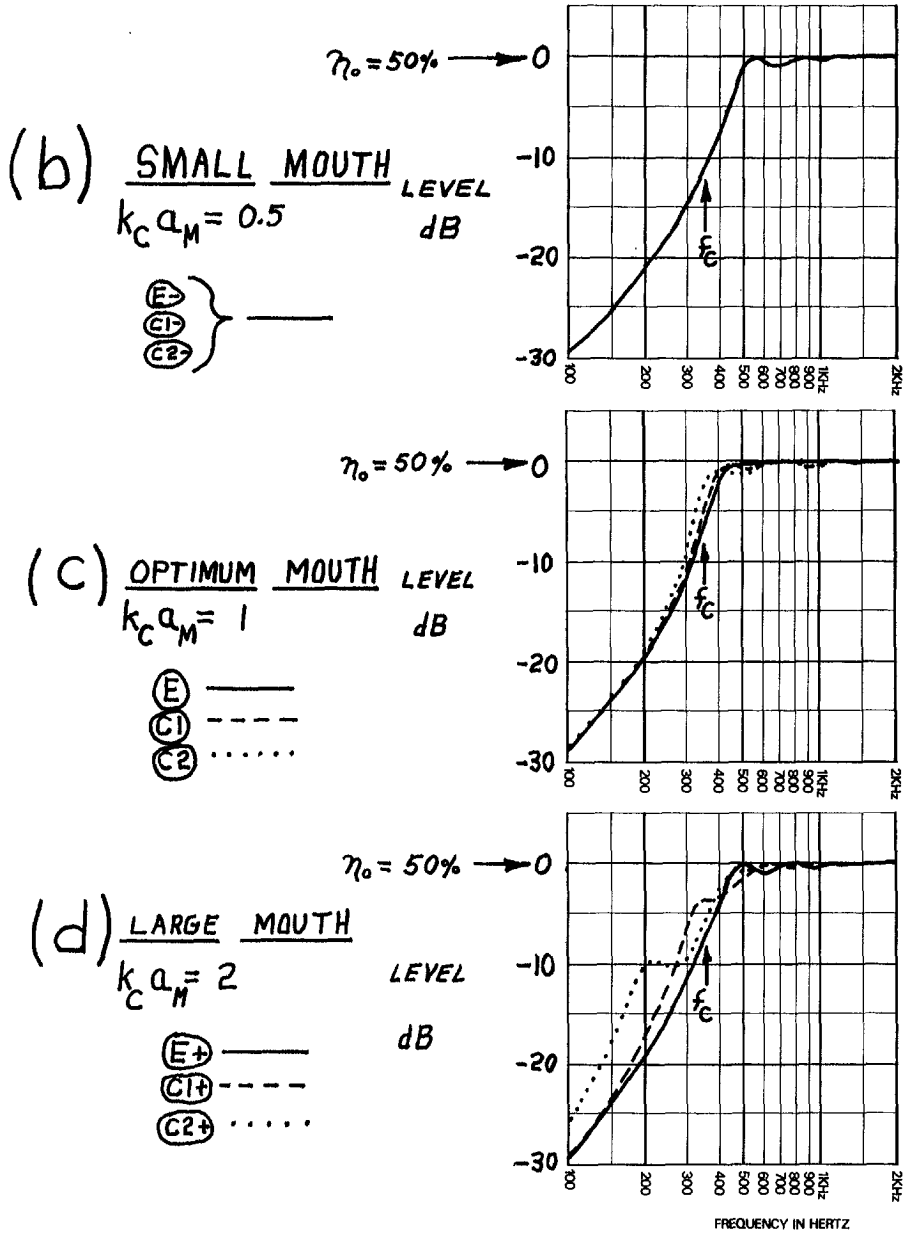

The efficiency comparisons for the three cases are shown in (b), (c) and (d). In general, the CE horn provides more output below cutoff and somewhat more passband ripple than its exponential prototype. The added response deviations are negligible for most practical cases.

CE HORN MOUTH FLARING

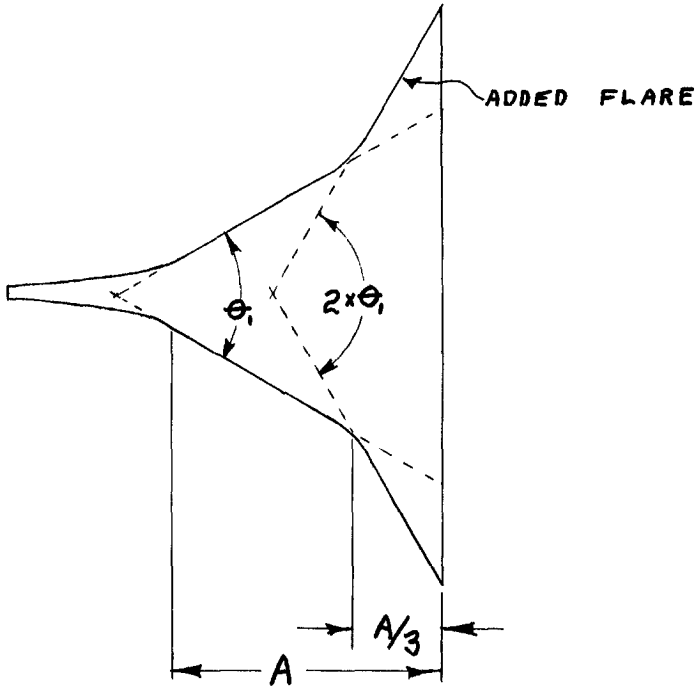

Fig. 16. Illustration of added flaring on mouth of conical-exponential horn which corrects midrange polar narrowing and polar lobing/fingering. Effective correction resulted when approximately the last third of the conical section was moved outward to roughly double the included angle.

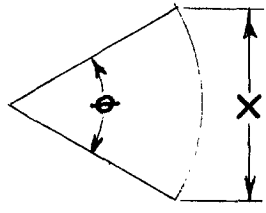

Fig. 17. Depiction of a generalized horn (in one plane only) which provides coverage angle θ and maximum mouth dimension X.

θ = coverage angle of horn (assumed to be the same as the included angle between the horn's sidewalls),

f_I = intercept frequency down to which coverage angle is maintained, and

K = a constant (=2.5 x 10^4 m-deg-Hz, or 1 x 10^6 in.-deg-Hz).

Eq. (1) applies to a broad class of horns which simulate radially vibrating sphere sections or arcs, including the multicell, radial (horizontal coverage only) and the new CE horn.

Fig. 18 graphically displays eq. (1). Note the large mouth sizes required for narrow coverage angle horns which operate down to relatively low frequencies. For example, a horn of 20° coverage angle required to operate down to 500 Hz must be about 2.5 meters (100 in.) wide.

For rectangular coverage area horns, a further relationship holds between the coverage angles, sizes and intercept frequencies. Analysis yields

$$A = \frac{X_H}{X_V} = \frac{\sin \frac{\theta_H}{2}}{\sin \frac{\theta_V}{2}} \qquad (2)$$

where A is the horn mouth height-width aspect ratio. If θ_H and θ_V are limited to a maximum of 120° eq. (2) is approximately

$$A \approx \frac{\theta_H}{\theta_V} \qquad (3)$$

Eq. (3) indicates that the mouth aspect ratio is fixed once the coverage angles are selected. i.e. a 40° x 20° horn would have a 2:1 mouth ratio etc.

Substituting eq. (1) for X_H and X_V into eq. (3) and solving for the ratio f_{IV}/f_{IH} yields

$$\frac{f_{IV}}{f_{IH}} \approx \left(\frac{\theta_H}{\theta_V}\right)^2 \qquad (4)$$

Eq. (4) governs the ordering and ratio of the intercept frequencies once the coverage angles are selected. For the 40° x 20° horn example, this means that upper intercept frequency will be four times higher than the lower frequency.

PRODUCT APPLICATION:

The CE horn theory discribed in this paper was applied to the design of three high frequency (400 to 16,000 Hz) rectangular coverage horns. Nominal

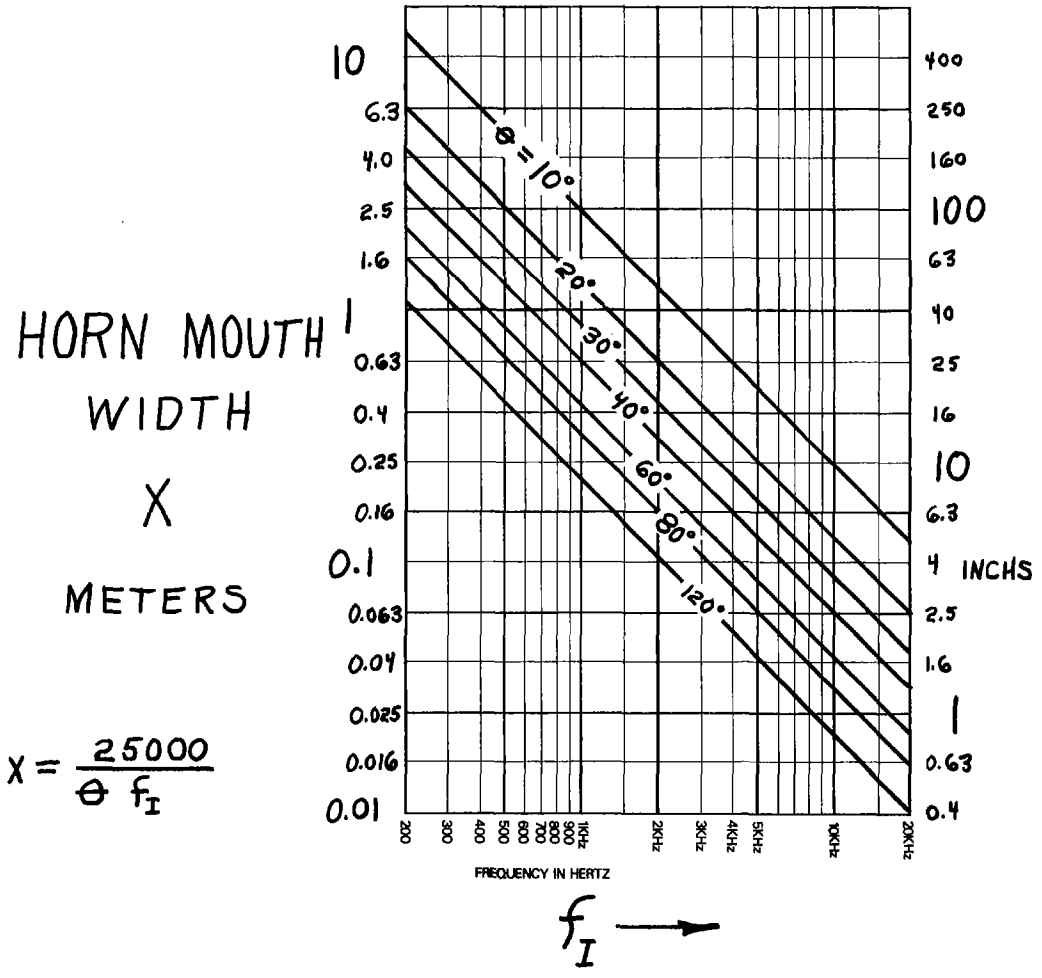

Fig. 18. Graph showing relationship between horn mouth width (or height) X, coverage angle θ and intercept frequency f_I. For a specific combination of θ and X the horn provides beamwidth control only down to f_I (see Fig. 1).

coverage angles were chosen to match existing sound industry radial and multicell horns. Coverage combinations targets of 90^{o} x 40^{o}, 60^{o} x 40^{o} and 40^{o} x 20^{o} were selected (θ_H x θ_V, horizontal by vertical respectively). In every case, maintenance of vertical beamwidth down to about 2 kHz (f_{IV} = 1.6 kHz) and horizontal beamwidth to 500 Hz was desired.

Computer model studies indicated that the exponential portion of the horn should be of the hyperbolic type with T = 0.6 and cutoff frequency of 360 Hz. The initial throat diameter of 1.3 inches was chosen to match a new Electro-Voice H.F. driver.

The desired rectangular coverage was developed by a combination of horizontal and vertical flaring which is very similar to the radial design. A short initial throat section of 0.5 inch provides a transition region where the crossection changes from circular to rectangular. From this point on the horizontal flaring is wedge shaped with straight sides angled at the desired horizontal coverage angle (except for mouth flaring). The vertical dimension varies so as to maintain the overall hyperbolic-exponential flare in the first part of the horn.

For the chosen angles and cutoff frequencies, the change from exponential to conical flare occurs at about 5 to 11 inches from the start of the horn, Beyond this coupling region, the vertical expansion is a straight sided wedge shape with included angle equal to the chosen vertical coverage angle. Fig. 19 shows horizontal and vertical crossections of each of the three horn designs.

Fig. 20 displays measured beamwidth, directivity factor (R_θ), and off-axis response curves for each design. These measurements were derived from one-third octave horizontal/vertical polar responses run in EV's anechoic chamber. The polar curves for each horn are displayed in appendix 3. R_θ was computed by a method discribed by Davis [5] and Wilson [6]. All off-axis response curves are referenced to the on-axis level. Note the constant directivity and beamwidth above 1.6 kHz for these designs.

Constant directivity in a horn implies that an axial frequency response with a particular driver should be in close correspondence to that driver's power response. This was checked on the 90^{o} design by equalizing flat the power response of a driver (from 200 Hz to 15 kHz) and then using that driver with EQ and running a 3 meter on-axis horn response curve. The results of these tests are shown in Fig. 21.

Fig. 21a shows the equalized power response of the driver as measured on a 6.1 meter terminated tube. The axial response of the 90^{o} horn with this driver attached (same EQ as in Fig. 21a) is shown in Fig. 21b. The horn's directivity index is also plotted, with the same scale, for reference purposes in Fig. 21c. Comparison of Figs. 21b and c indicates good correspondence.

40°x20° CE HORN

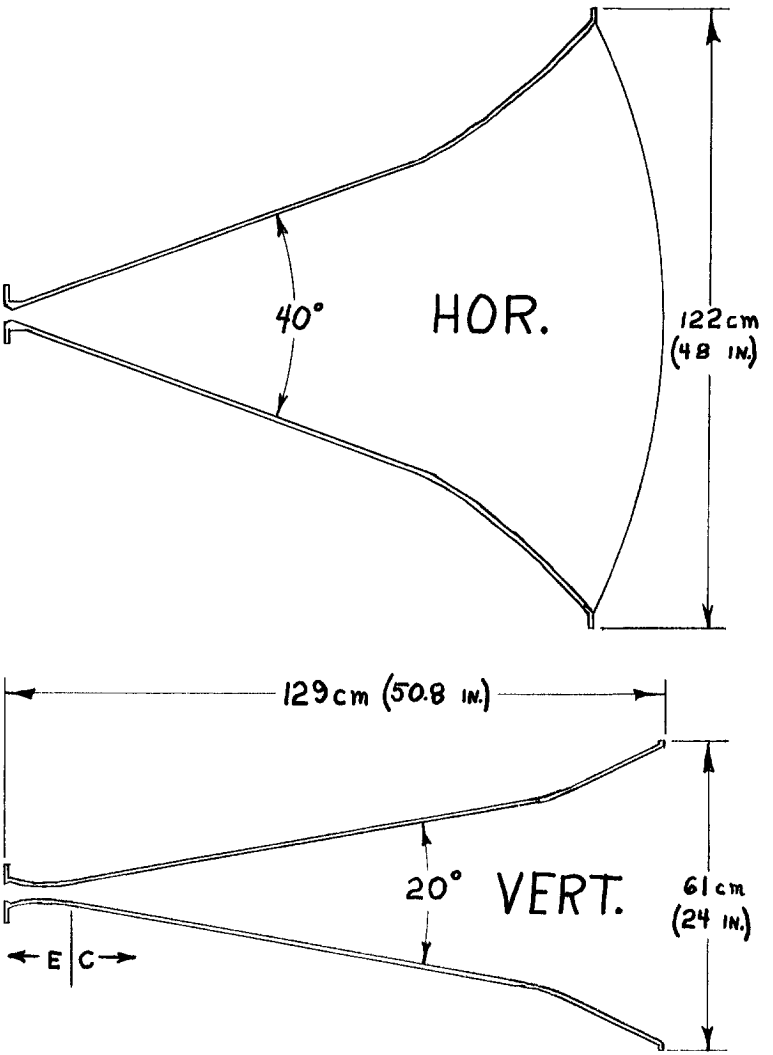

Fig. 19a. Horizontal and vertical contour sketchs of the 40° x 20° coverage long-throw conical-exponential (CE) horn (EV model HR4020). The transition from exponential (f_C = 360 Hz, T = 0.6) to conical occurs at 12.7 cm (5 in.) from the start of the horn.

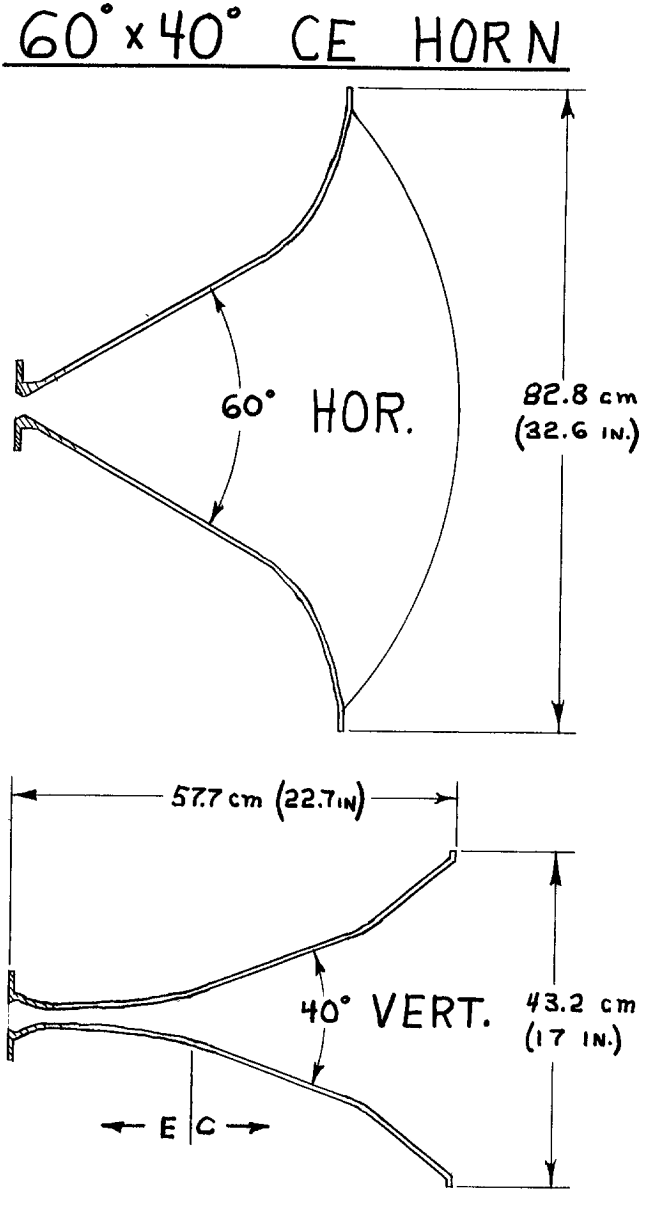

Fig. 19b. Sketches of horizontal and vertical contours of the 60° x 40° medium-throw CE horn (EV model HR6040). The switch from exponential to conical occurs at 23.6 cm (9.3 in.) from the start of the horn.

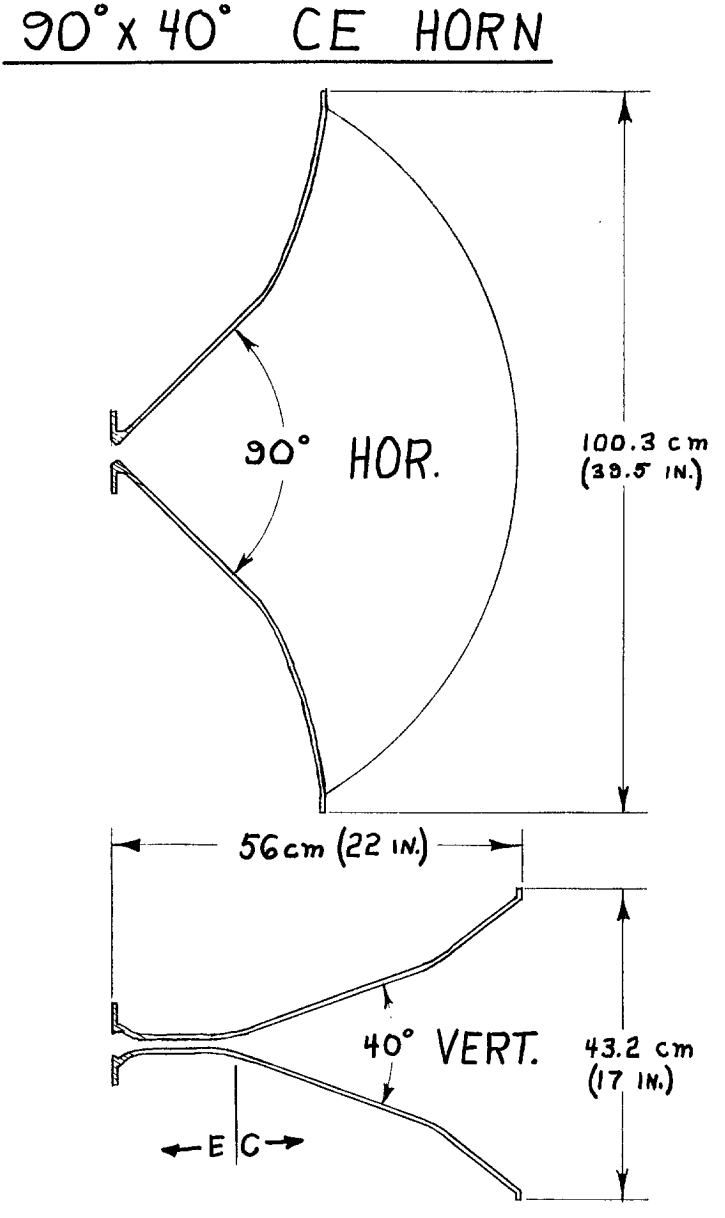

Fig. 19c. Contour sketches of wide angle 90° x 40° coverage CE horn (EV model HR9040). Change to conical occurs at 16.5 cm (6.5 in.) from horn start.

BEAMWIDTH IN DEGREES (-6dB) (LOG SCALE)

DIRECTIVITY FACTOR R_θ (Q)

40°x20° HORN	60°x40° HORN	90°x40° HORN
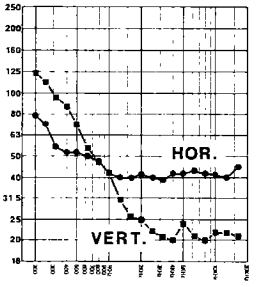	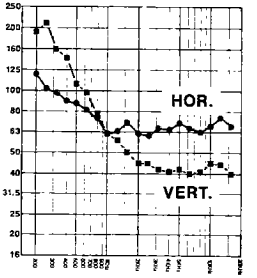	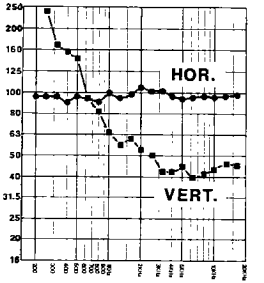
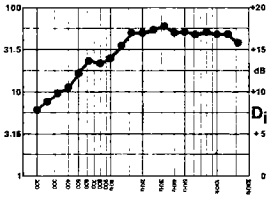	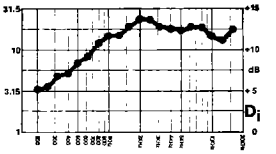	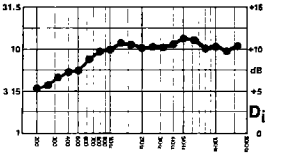
Directivity Factor R_θ (Q) 48.7 (+10.4, −12.6) (average 1.25 kHz to 16 kHz) Directivity Index D_i 16.9 dB (+.8 −1.3 dB) (10 Log R_θ, average 1.25 kHz to 16 kHz)	Directivity Factor R_θ (Q) 17.7 (+6.3, −5.6) (average 800 Hz to 16 kHz) Directivity Index D_i 12.5 dB (+1.3, −1.7 dB) (10 Log R_θ, average 800 Hz to 16 kHz)	Directivity Factor R_θ (Q) 10.9 (+2.5, −1.5) (average 800 Hz −16 kHz) Directivity Index D_i 10.4 dB (+.9, −.6 dB) (10 Log R_θ, average 800 Hz to 16 kHz)

Fig. 20a. Display of beamwidth and directivity factor/index measurements on the three horns shown in Fig. 19. Note both the well behaved beamwidth and the uniform directivity of these designs (compare with Figs. 2 and 3). These curves were derived from the measured one-third octave polar responses taken on the horns which are shown in appendix 3.

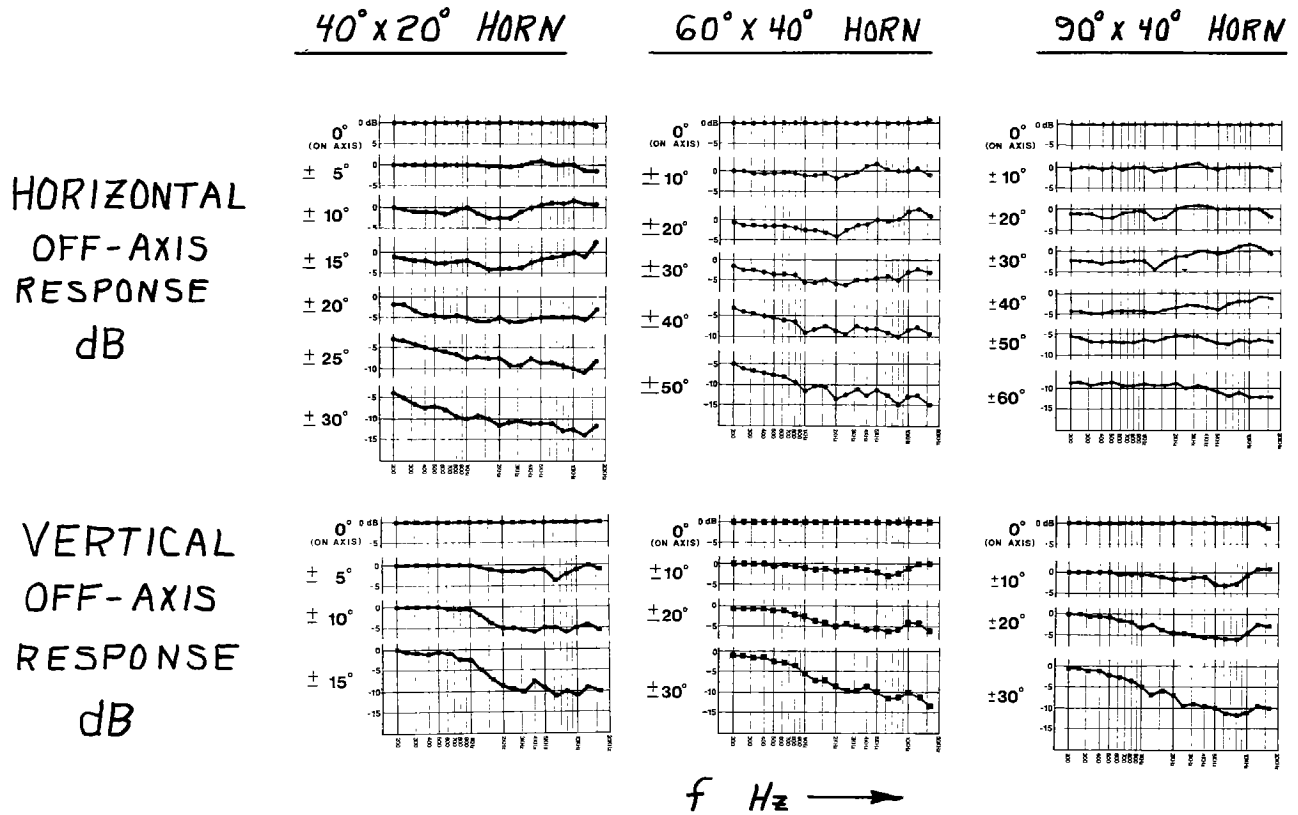

Fig. 20b. Display of one-third octave frequency response curves on the three horns of Fig. 19 taken at selected off-axis angles. These curves were derived from the polars shown in appendix 3. Each curve is referenced to the on-axis level. The curves shown here indicate the direct-field frequency response one would get at various off-axis angles with a one-third-octave real-time spectrum analyzer, if the horn/driver were equalized flat on axis. The relatively good off-axis response curves on these horns is a direct result of the uniform non-lobing nature of the polar responses.

(a)

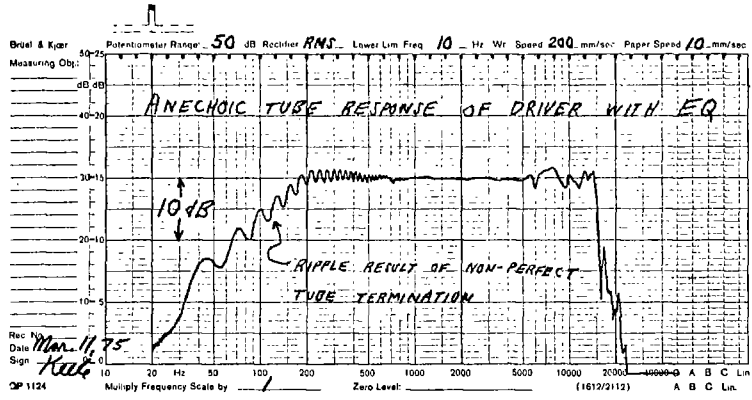

(b)

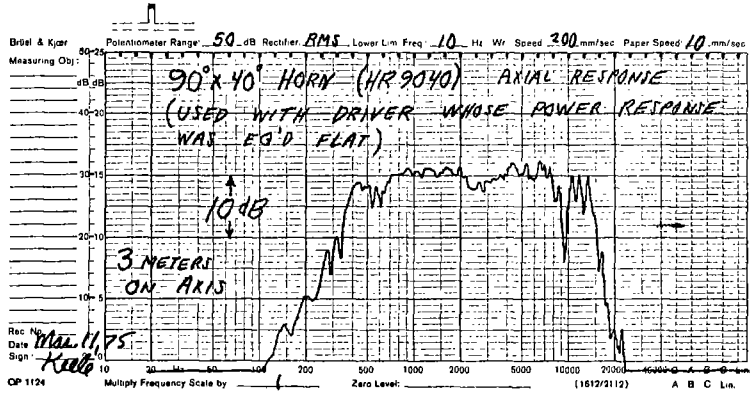

(c)

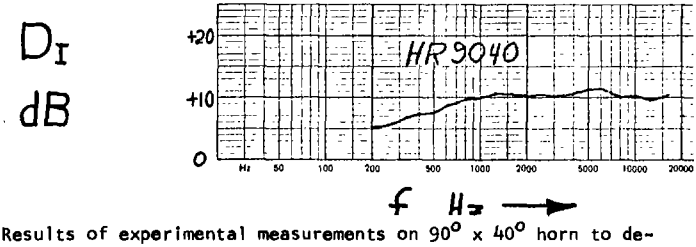

Fig. 21. Results of experimental measurements on 90° x 40° horn to determine transmission characteristics when used with driver which has a flat power output response curve. (a) shows the driver's power frequency response as measured on a 6.1 meter anechoic pipe and equalized with a one-third octave equalizer (1/8 inch Bruel and Kjaer mic). The HR9040's axial frequency response taken at 3 meters with the equalized response driver attached is shown in (b). For comparison, the directivity index vs. frequency of the HR9040, plotted on the same scale, is shown in (c).

It should be noted that the designs bear a resemblance, except for mouth flaring and absence of internal baffles, to a horn design patented some thirty years ago by Klipsch [7]. The rectangular coverage implementation of the CE horn is similar to Klipsch's design in that a form of wavefront "astigmatism" is generated. This arises because the vertical wavefront radius of curvature is different from the horizontal radius. From a practical standpoint, this astigmatism appears to be of no consequence whatsoever.

CONCLUSION:

A new class of horns which exhibit very constant directivity and beamwidth have been discribed. These horns optimally join a modified conical flare with an exponential flare throat section. The good low frequency response of the exponential horn is retained while the conical flare provides excellent pattern control. The angular radiation characteristics are found to be much better than the exponential multicellular horn but without the complex internal cell/baffle arrangement. The new class of horns provide a very wide design margin in selection of designed horizontal and vertical coverage angles.

REFERENCES

[1] V. Salmon, "A New Family of Horns," J. Acoust. Soc. Am., vol. 17, p. 212 (January 1946).

[2] H. F. Olson, Acoustical Engineering (D. Van Nostrand Co., New York, 1960).

[3] L. L. Beranek, Acoustics (McGraw-Hill, New York, 1954).

[4] D. B. Keele, Jr., "Optimum Horn Mouth Size," presented at the 46th Audio Eng. Soc. Convention, Preprint No. 933 (B-7) (September 1973).

[5] D. Davis, "On Standardizing the Measurement of Q," J. Audio Eng. Soc., vol. 21, pp. 730-731 (November 1973).

[6] G. L. Wilson, "Directivity Factor" Q or R_θ? Standard Terminology and Measurement Methods," J. Audio Eng. Soc., vol. 21, pp. 828-833 (December 1973).

[7] P. W. Klipsch, "Loudspeaker Horn," United States Patent, No. 2,537, 141 (January 1951) (Application date June 1945).

APPENDIX 1

THE MATCHED ACOUSTIC SOURCE

A relatively easy way of comparing different horn flares, with respect to efficiency and frequency response, uses the concept of the matched acoustic source. The matched acoustic source is an acoustic generator with a source conductance (volume velocity/pressure) of

$$G_S = \frac{S}{\rho_o c} \qquad (5)$$

where

G_S = source conductance,

ρ_o = density of air (=1.21 kg/m^3)

c = speed of sound in air (=343 m/s), and

S = crossectional area of acoustic source.

When this generator is used to drive an acoustic load impedance Y_L with the same area S, a power available efficiency can be defined

$$\eta_o = \frac{2\, G_S\, G_L}{(G_S + G_L)^2 + B_L^2} \qquad (6)$$

where

η_o = power available efficiency,

G_S = source conductance (=$S/(\rho_o c)$),

G_L = real part of acoustic load admittance,

B_L = complex part of acoustic load admittance and

$Y_L = G_L + jB_L$ = acoustic load admittance

Note that the power available efficiency assumes a value of 0.5 or 50% when the load is an infinite pipe of area S (characteristic admittance of $S/(\rho_o c)$). The transformation between acoustic impedance Z_a and admittance Y_a is $Y_a = 1/Z_a$.

The matched source can be thought of as simulating an ideal driver of zero moving mass and infinite suspension compliance. The simulated driver's Bl product, coil resistance and diaphragm area are chosen so as to yield 50% efficiency (motional impedance one-half of input impedance) when it drives an infinite tube of the same diameter as the horns throat.

APPENDIX 2

OPTIMUM FLARE JOINING

The conical and exponential flares were joined together in a manner which minimizes internal reflections at the junction point between the two flares. This was accomplished by selecting the junction point to minimize the junction reflection coefficient over a selected band of frequencies. This specific case was analyzed is some detail in a previous paper [4].

For a circular crossection exponential horn of cutoff frequency f_c, feeding into a conical horn of solid angle Ψ, the following radius at the junction point was found to minimize internal reflections over the range f_c to 10 f_c:

$$a_J = \frac{0.95 \sin \theta}{k_c} \qquad (7)$$

where

a_J = radius at junction point,

θ = half angle of cone with solid angle Ψ $\left(= \cos^{-1}\left(1 - \frac{\Psi}{2\pi}\right)\right)$,

$k_c = 2\pi/\lambda_c = 2\pi f_c/c$,

f_c = exponential horn cutoff frequency, and

c = speed of sound.

Once the junction radius is computed by eq. (7), it is a simple matter to compute the junction distance from the start of the exponential horn by the use of the exponential horn equation.

APPENDIX 3

HORN POLAR CURVES

The directional characteristics of each of the three horn designs (with driver attached) were measured by running a set of horizontal/vertical polar responses, in EV's large anechoic chamber, at each one-third octave center frequency. The test signal was one-third octave bandwidth limited pseudo-random pink noise (1 Hz rep rate) centered at the indicated frequencies. The measurement microphone was placed 3.5m (11.5 ft) (4.5m for the HR4020) from the horn mouth, while rotation was about the horn rear driver flange. The horn was suspended freely with no baffle.

The following polars show the results of these tests. The effects of the pseudo-random noise are clearly shown in the cyclic variations of level with angle. The beamwidth angles and center frequencies are noted on each polar. At each frequency, the horizontal and vertical polars have been superimposed. The curves may be separated by comparing each beamwidth marked curve to the beamwidth angle numbers printed in the center of each polar. The horizontal beamwidth number is listed on top in every case.

40°x20° HORN POLAR RESPONSE

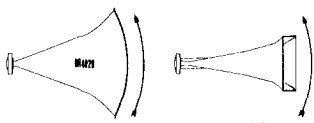

SCALE IS 5 DECIBELS PER DIVISION

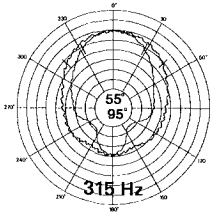

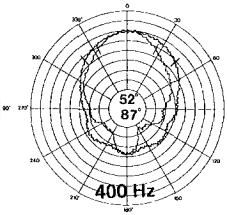

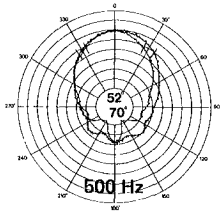

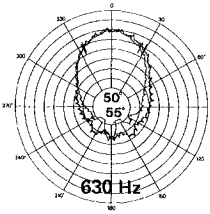

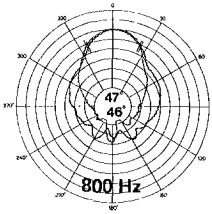

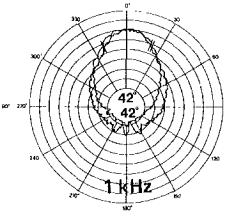

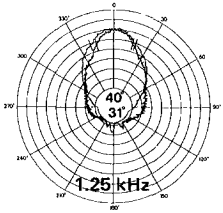

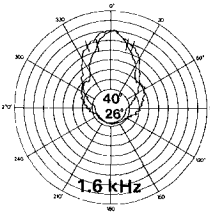

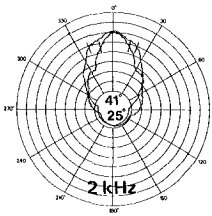

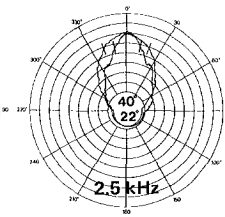

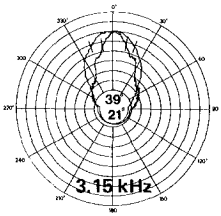

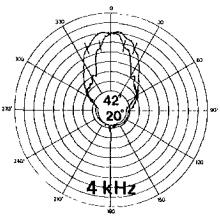

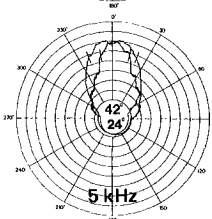

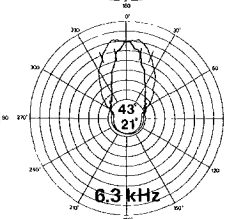

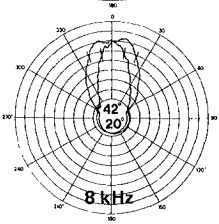

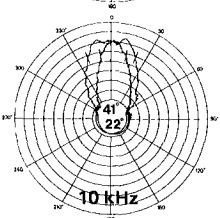

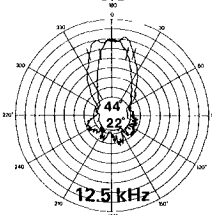

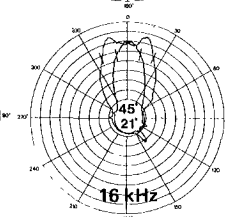

60° x 40° HORN POLAR RESPONSE

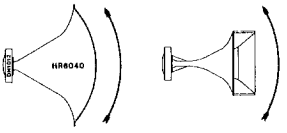

HORIZONTAL VERTICAL

SCALE IS 5 DECIBELS PER DIVISION

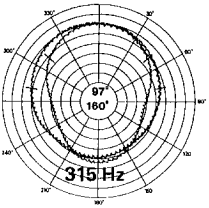

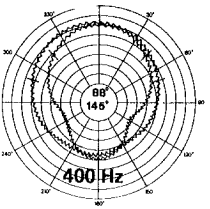

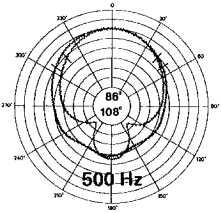

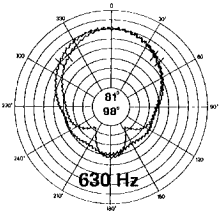

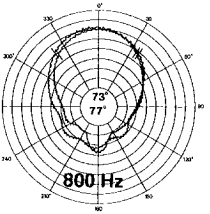

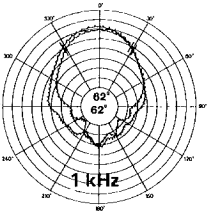

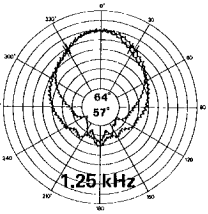

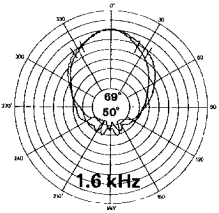

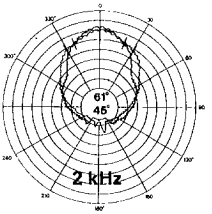

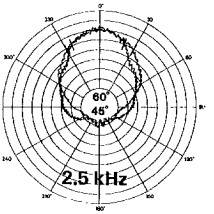

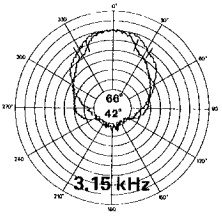

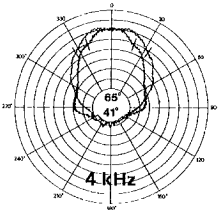

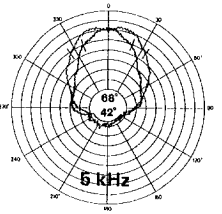

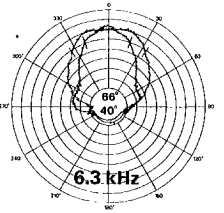

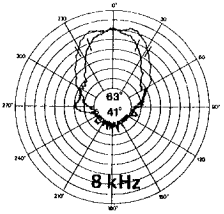

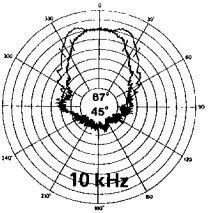

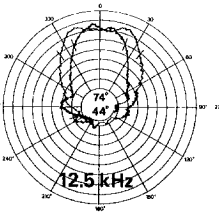

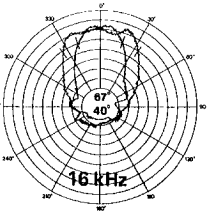

90° x 40° HORN POLAR RESPONSE

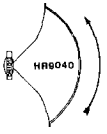

HORIZONTAL

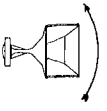

VERTICAL

SCALE IS 5 DECIBELS PER DIVISION